Protein Kinase C Phosphorylation Modulates N- and C-Terminal Regulatory Activities of the PITX2 Homeodomain Protein†

Herbert M. Espinoza,‡ Mrudula Ganga,‡ Usha Vadlamudi,‡ Donna M. Martin,§ Brian P. Brooks,|| Elena V. Semina,⊥ Jeffrey C. Murray,# and Brad A. Amendt*,‡

Department of Biological Science, The University of Tulsa, Tulsa, Oklahoma 74104-3189, Department of Pediatrics and Human Genetics, University of Michigan Medical Center, Ann Arbor, Michigan 48109-0652, National Eye Institute, National Institutes of Health, Bethesda, Maryland 20892, Department of Medical Genetics, Medical College of Wisconsin, Milwaukee, Wisconsin, 53226, and Department of Pediatrics, The University of Iowa, Iowa City, Iowa 52242

Received July 30, 2004; Revised Manuscript Received October 20, 2004

ABSTRACT: PKC phosphorylation regulates PITX2 DNA binding and transcriptional activity. Mutation of individual PKC sites demonstrates the functional regulation of PITX2 through phosphorylation. Immunoprecipitation of PITX2 and a PITX2 PKC mutant protein reveal specific in vivo phosphorylation by PKC in transfected cells. The transcriptional activity of PITX2 is negatively regulated by N-terminal phosphorylation and positively regulated by C-terminal phosphorylation. We demonstrate a mechanism of increased PITX2 transcriptional activation through protein interactions facilitated by phosphorylation of the PITX2 C-terminal tail. Phosphorylation of the PITX2 C terminus enhances the interaction with cellular factors. In corroboration with the PITX2 PKC functional studies, a newly identified C-terminal *PITX2* mutation associated with Axenfeld−Rieger syndrome (ARS) demonstrates reduced phosphorylation. This mutation (*PITX2* Δ*T1261*) creates a frameshift mutation in codon 227 resulting in 11 novel amino acids downstream followed by premature truncation of the protein. Three PKC sites in the C-terminal tail and OAR domain are deleted, which results in decreased transcriptional activation. PITX2 ΔT1261 is unable to interact with a cellular factor to synergistically activate transcription and demonstrates the first link of ARS with defective PITX2 protein interactions. Gene expression profiling of homozygous *Pitx2* mutant mouse tissue reveals decreased *Dlx2* expression as a potential molecular basis for developmental defects associated with ARS patients. Overall, phosphorylation imparts another level of regulation to the activity of the PITX2 homeodomain protein during development.

Pitx2, a *paired*-like homeodomain gene, is expressed in the brain, heart, pituitary, mandibular and maxillary regions, eye, and umbilicus and is required for normal embryonic development (*1*−*13*). Many genes have been identified that are regulated by PITX2 (*14*−*23*). Previous results reveal both promoter and cell dependent activation by the three major PITX2 isoforms (*24*). The recent identification of a fourth *PITX2* isoform (*PITX2D*) expressed only in humans acts to repress the activity of the other PITX2 isoforms and adds another level of regulation to the transcriptional activity of PITX2 (*24*). In the human brain, craniofacial region, and pituitary, which express all PITX2 isoforms (Hjalt, personal communication), the interactions between PITX2 isoforms would provide a mechanism to tightly regulate gene expression. Dimerization between PITX2 isoforms can either inhibit or synergistically activate gene expression (*18*, *20*, *24*, *25*). Thus, the levels and combinations of PITX2 isoform expression would contribute to the dosage-response model proposed for pituitary and other organ development (*11*, *26*, *27*). Because Axenfeld−Rieger syndrome (ARS)[1] is a haploinsufficiency disorder associated with *PITX2* mutations, reduced levels of *PITX2* expression are causative for the phenotypes observed in these patients (*28*, *29*). However, other mechanisms likely contribute to the transcriptional regulation of gene expression by PITX2 during development.

One of these mechanisms includes protein phosphorylation. Protein phosphorylation can induce rapid modulation of transcriptional activity, providing three main levels of regulation. Phosphorylation can affect the DNA binding activity of transcription factors, their subcellular localization, or their interaction with the transcription machinery (*30*−*34*). Among the kinases that control these processes, PKC plays an important role in the transduction of growth factor

† Support for this research was provided from Grants DE 13941 from the National Institute of Dental and Craniofacial Research to B.A.A. and EY12384 to J.C.M.

* To whom correspondence should be addressed. Mailing address: Department of Environmental and Genetic Medicine, The Texas A&M University System, Health Science Center, Institute of Biosciences and Technology, 2121 W. Holcombe Boulevard, Houston, TX 77030-3303. Tel: 713-677-7402. Fax: 713-677-7427. E-mail: bamendt@ibt.tamhsc.edu.

‡ The University of Tulsa.

§ University of Michigan Medical Center.

|| National Institutes of Health.

⊥ Medical College of Wisconsin.

The University of Iowa.

[1] Abbreviations: PKC, protein kinase C; PMA, phorbol 12-myristate 13-acetate; BIM, bisindolylmaleimide; PKA, protein kinase A; CKII, casein kinase II; CMV, cytomegalovirus; SDS, sodium dodectl sulfate; EMSA, electrophoretic mobility shift assay; PCR, polymerase chain reaction; GST, glutathione S-transferase; PVDF, polyvinylidene difluoride; HD, homeodomain; NE, nuclear extract; ARS, Axenfeld−Rieger syndrome; Luc, luciferase; DMEM, Dulbecco's modified Eagle's medium; FBS, fetal bovine serum.

10.1021/bi048362x CCC: $30.25
Published on Web 02/15/2005

signals that lead to either positive or negative changes in gene expression, cell growth, and differentiation.

There are twelve isozymes of PKC in mammalian tissues: conventional PKC members, α, *β*I, *β*II, and *γ* isoforms (activated by calcium, acidic phospholipid, diacylglycerol (DAG), and phorbol esters), novel PKC isoforms, *δ*, *ϵ*, *η*, and *θ* (activated by DAG, and acidic phospholipid), and atypical PKCs, *ι*/*λ*, *ζ*, and *μ* (*35*−*41*). PKC isoforms exhibit small differences in their dependencies on lipid cofactors and overlapping substrate specificities; however, a major distinguishing feature of PKC isoforms is their distinct tissue and cellular localization (*42*, *43*). The specific substrate sequence motifs of the PKC isozymes have been analyzed using synthetic peptides and known protein sequences (*43*, *44*). Comparison of the ten PKC sites in PITX2A correlates with sites predicted for the classical PKC α, *β*I, *β*II, and *γ* isoforms (*43*, *44*). Furthermore, the tissue distributions of these isoforms correlate with *Pitx2* expression.

We have focused on the PITX2A isoform to demonstrate specific phosphorylation by PKC. The DNA binding and transcriptional activities of the PITX2A isoform have been extensively studied and is important in development (*1*, *15*). PITX2A is phosphorylated through ten consensus PKC sites; 3 sites are located within the N-terminus, 2 sites are within the homeodomain, and 5 sites are located in the C-terminus. The functional activity of each phosphorylation site is revealed through mutation of the individual PITX2A PKC sites. PITX2A N-terminal phosphorylation acts to inhibit its transcriptional activity while C-terminal phosphorylation increases transcriptional activity. C-Terminal phosphorylation facilitates transcriptional synergy with the Pit-1 homeodomain protein. Furthermore, we provide a molecular basis for a new and novel C-terminal *PITX2* mutation through disrupted phosphorylation and protein interactions as a cause for the developmental defects seen in this ARS patient (*45*). This is the first report of ARS developmental defects caused by defective PITX2 protein interactions.

In addition, our tissue expression studies reveal that *Dlx2* expression is down regulated in *Pitx2* mutant mice. We demonstrate through our in vitro and in vivo studies that *Dlx2* is regulated by PITX2, which is modulated by PKC phosphorylation, and these data provide support for the transcriptional influences of Pitx2 on *Dlx2* expression in the mouse embryo during development.

MATERIALS AND METHODS

Expression and Reporter Constructs. Expression plasmids containing the cytomegalovirus (CMV) promoter linked to the *PITX2A* DNA were constructed in pcDNA 3.1 MycHisC (Invitrogen) (*15*, *18*). Specific PITX2A point mutations to generate the PKC site mutations were made using the two-step megaprimer PCR technique (*15*). To make plasmid PITX2A PKC Δ9−10, which has point mutations at position 258 (serine to alanine) and position 237 (serine to glycine), a sense primer (5′-CTGGCCGGCCTAAGACTGAAA-3′) and antisense primer with *Hin*DIII site (5′-CCCATTAAGCTTCACGGGCCGGTCCACTGCATACTGGCAAGCACTCAGGTTGGCGGCCGGTTTCTG-3′) were used in the first PCR reaction. The specific base mutations are underlined. The megaprimer was purified and used as the antisense primer for the second step. The megaprimer was combined with a sense primer containing a *Bam*HI site (5′-CGGGATCCCGCCGATAACGGGGAAATGGAG-3′). The PCR product was digested with *Bam*HI and *Hin*DIII and ligated into the pcDNA 3.1 MycHisC vector and is in frame with the Myc and His epitopes. This plasmid was used as a template to make PITX2A PKC Δ8−10. The first PCR reaction contained the sense primer (5′-TCGAGCCTGGCCGGCCTGGCGTGTAAC-3′), which changed the threonine at position 230 to an alanine (base change is underlined) and the antisense primer containing a *Hin*DIII site (5′-CCCATTAAGCTTCACGGGCCGGTCCACTGCATACT-3′) was used to make the megaprimer. The second step contained the megaprimer and the previous sense primer. This plasmid (PITX2A PKC Δ8−10) was used as a template to make PITX2A PKC Δ6−10. The first PCR reaction contained the sense primer (5′-AAGGGCCTTGCATCCGCCTCCCTAGCCACCAAGAGC-3′), which changed the threonine at position 139 to an alanine and the serine at position 144 to an alanine (base change is underlined), and the previous *Hin*DIII antisense primer. The megaprimer was used with the *Bam*HI sense primer to generate the complete PCR product. This clone termed PITX2A PKC Δ6−10 has all five C-terminal PKC sites mutated. This plasmid was used as a template to make PITX2A PKC Δ5−10. The first PCR reaction contained the antisense primer (5′-TTCTTCGCGTGTGGCCATGTCCGG-3′), which changes the serine at position 67 to an alanine (base change underlined), and the previous *Bam*HI sense primer. The megaprimer was combined with the *Hin*DIII antisense primer to generate the full-length PCR product and cloned into the vector. To make PITX2A PKC Δ5 the same procedure was performed only using wild-type PITX2A as the template DNA. This plasmid has only the central homeodomain PKC site #5 mutated. To make plasmid PITX2A PKC Δ1−2, which has the first two N-terminal PKC sites mutated, the sense primer with *Bam*HI site (5′-GCGGGATCCCGAACGGGGAAATGGAGACCAACTGCCGCAAACTGGTGGCGGCGTGTCTGCAATTAGAGAAAGATAAAGGCCAGCAG-3′) was used and changes the serine at position 10 to an alanine and the serine at position 20 to a glycine (base changes are underlined). The antisense primer was the *Hin*DIII primer described above, and the template was wild-type PITX2A. This plasmid (PITX2A PKC Δ1−2) was used as the template to make plasmid PITX2A PKC Δ1−4. The first PCR reaction contained the antisense primer (5′-AAAGTGAGCCCGCTGCCGCCTTTGCCGCTTCTTCTTAGCCGGGTC-3′), which changes the serine at position 34 to an alanine and the threonine at position 44 to an alanine (base changes are underlined), and the *Bam*HI sense primer. The megaprimer was then used as a sense primer with the *Hin*DIII antisense primer to generate the full-length PCR product. This clone (PITX2A PKC Δ1−4) was used as the template to make PITX2A PKC Δ1−5. The first PCR reaction contained the *Bam*HI sense primer and the PKC Δ5 antisense primer to make the megaprimer, which was used as the sense primer in the second step. The megaprimer was combined with the *Hin*DIII antisense primer to generate the full-length product. To make plasmids PITX2A PKC Δ1−4, 6−10, and PITX2A PKC Δ1−10, combinations of the appropriate megaprimers and templates were used. All PCR reactions were performed as previously described (*15*). The *prolactin* and *Dlx2* promoter luciferase plasmids have been previously described

(*18*, *20*). To make the C-terminal mutation termed PITX2A ΔT1261, the sense primer (5′-TCCTCCGTATGTTATAGGGACACG-3′) and antisense primer (5′-CGTGTCCCTATAACATACGGAGGA-3′) were used with the mutagenesis kit protocol. All constructs were confirmed by DNA sequencing. A CMV β-galactosidase reporter plasmid (Clontech) was cotransfected in all experiments as a control for transfection efficiency.

Western Blot Assays. Expression of transiently expressed PITX2 proteins was demonstrated using the PITX2 antibody (*19*). Approximately 10 μg of transfected cell lysates was analyzed in Western blots. Following SDS gel electrophoresis, the proteins were transferred to PVDF filters (Millipore), immunoblotted, and detected using PITX2 antibody P2R10 and ECL reagents from Amersham.

Cell Culture, Transient Transfections, Luciferase, and β-Galactosidase Assays. CHO, LS-8, GH3, and HeLa cells were cultured in Dulbecco's modified Eagle's medium (DMEM) supplemented with 5% or 10% fetal bovine serum (FBS) and penicillin/streptomycin in 60 mm dishes and transfected by electroporation. CHO and HeLa cells were mixed with 2.5 μg of expression plasmids, 5 μg of reporter plasmid, and 0.5 μg of CMV β-galactosidase plasmid plated in 60 mm culture dishes and fed with 5% FBS and DMEM. Electroporation of CHO cells was at 360 V and 950 microfarads (μF) (Bio-Rad); cells were fed 24 h prior to transfection. HeLa cells were transfected by electroporation at 220 V and 950 μF, and cells were fed 24 h prior to transfection. Phorbol 12-myristate 13-acetate (PMA) activation of PKC was performed after transfection by adding 50 ng/mL to the culture medium. Bisindolylmaleimide (BIM) inhibition of PMA stimulation was performed after transfection by adding BIM (100 nM) immediately after transfection followed by PMA treatment. PKI (Promega) inhibition of PKC activity was performed after transfection by adding PKI (50 μM) immediately after transfection. Transfected cells were incubated for 24 h, then lysed, and assayed for reporter activities and protein content by Bradford assay (BioRad). Luciferase was measured using reagents from Promega. β-Galactosidase was measured using the Galacto-Light Plus reagents (Tropix Inc.). All luciferase activities were normalized to β-galactosidase activity.

Expression and Purification of GST-PITX2A Fusion Proteins. The human *PITX2A*, *PITX2A* mutations, PKC mutations, and deletion constructs were PCR amplified from cDNA clones as described (*15*, *18*). The *PITX2A* PCR products were cloned into the pGex6P2 GST vector (Amersham Pharmacia Biotech) as previously described (*15*, *18*). The plasmids were transformed into BL21 cells. Protein was isolated as described (*15*). PITX2A proteins were cleaved from the GST moiety using 80 units of PreScission Protease (Pharmacia Biotech) per mL of glutathione Sepharose. Purified proteins used in the binding assays have been previously described or reported in this manuscript (*18*). The cleaved proteins were analyzed on SDS polyacrylamide gels by silver stain or Coomassie blue stain and quantitated by the Bradford protein assay (BioRad). All stained gels were directly quantitated using image analysis programs.

Electrophoretic Mobility Shift Assay (EMSA) and Nuclear Extract Preparation. Complementary oligonucleotides containing a *Dlx2 bicoid* site with flanking partial *Bam*HI ends were annealed and filled with Klenow polymerase to generate ^{32}P-labeled probes for EMSAs, as described (*20*). Standard binding assays were performed as previously described (*18*). Either 80 or 160 ng samples of the bacterial expressed and purified PITX2A proteins were used in the assays. The samples were electrophoresed, visualized, and quantitated as described previously, except quantitation of dried gels was performed on the Molecular Dynamics STORM PhosphoImager (*15*).

Nuclear extracts (NE) were prepared from GH3, LS-8, and CHO cells using the mini extract protocol as previously described (*46*, *47*). Nuclear extracts were dialyzed against 50 mM NaCl with 2 changes of dialysis buffer.

Kinase Assays. PITX2A, PITX2A mutant, and PITX2A truncated protein concentrations were normalized to 0.5 μg of PITX2A to ensure equal protein concentrations and account for the size differences between truncated proteins and number of protein molecules. Samples were incubated in kinase buffer (50 mM Tris-Cl pH 8.0, 100 mM NaCl, 5 mM $MgCl_2$, 4 mM DTT), kinase (protein kinase A, PKA, Boehringer Mannheim, Indianapolis, IN; casein kinase II, CKII; or protein kinase C, PKC, Promega, Madison, WI), and γ-^{32}P-ATP (Amersham Pharmacia, Piscataway, NJ) for 30 min at 30 °C. Proteins were then separated by electrophoresis on a 12.5% polyacrylamide or tricine gel. Gels were exposed to imaging film (Kodak X-OMAT AR) and to a Phosphor screen for quantitation on the Storm 860 Phosphorimager system (Molecular Dynamics, Amersham Pharmacia, Piscataway, NJ). Kinase assays were also performed with 33 mM heparin sulfate and 1 μM bisindolylmaleimide (BIM, Sigma, St.Louis, MO) known inhibitors of casein kinase II and protein kinase C, respectively.

Endogenous Kinase Assays. PITX2A GST-fusion proteins on glutathione Sepharose 4B beads (Amersham Pharmacia) were incubated with nuclear extracts (~10 μg) in place of the commercially available kinases, at 37 °C for 30 min. Inhibitors were used to determine specific kinase activity. Beads were washed 4× with 100 μL kinase buffer and reconstituted in kinase buffer. Proteins were separated on a 12.5% SDS polyacrylamide gel. Analysis was evaluated on imaging film and by phosphorimaging.

Isolation of Mouse Tissue and RT-PCR Assays. Timed pregnancies were establish between adult male and female *Pitx2*$^{+/-}$ mice (generation N6−7) and embryos harvested, after cervical dislocation, into cold PBS (pH 7.4). The morning of plug identification was designated as embryonic day 0.5. E12.5 embryos were harvested, amniotic sacs were collected, and DNA was isolated and processed for genotyping using previously described PCR primers and conditions (*48*). Face tissues were removed by manually separating the nasal, maxillary, and mandibular prominences from more caudal and dorsal structures. Fresh tissues were homogenized and processed for RNA using Trizol (Invitrogen). Total RNA was isolated as previously described (*46*).

Reverse transcription was preformed using 1 μg of total RNA, random primers, and AMV RT (Takara Mirus Bio) in a total volume of 20 μL. The reaction mixture was incubated at 42 °C for 50 min. Products were analyzed on an agarose gel, and bands were isolated and sequenced to confirm their identity.

Real-time PCR was carried out using a Smart Cycler thermal cycler (Cepheid, Sunnyvale, CA). Separate cDNA reactions are used for each RNA preparation analyzed. Each

PCR reaction contains the appropriate components, and SYBR Green I (Epicenter Technologies). PCR cycling conditions were 94 °C for 1 min, 60 °C for 2 min, and 72 °C for 2 min. Optical data is collected during the annealing step. A melting curve was generated at the end of every run to ensure product uniformity. All primers were tested using standard RT-PCR protocols and the products sequenced to ensure and confirm their specificity. The *Dlx2* primers were previously described, and standard β-actin primers were used in the PCR reactions (*49*, *50*)

Optical data was exported from the Cepheid Smart Cycler as comma separated values files (*.csv) and imported into MS Excel. A Visual Basic Excel macro was used that facilitates determination and conversion of the appropriate Smart Cycler optics data to a logarithmic format for subsequent analysis (*51*). Ct values were obtained from 3 separate experiments, and the *Dlx2* expression values were normalized to *β-actin* values for each preparation. The normalized values from the *Pitx2* homozygous mouse were compared to the wild-type mouse. The differences in Ct values are shown as fold-decrease in transcript levels (*51*).

Immunoprecipation Assays. CHO cells were transfected with 5 μg of either PITX2A, PITX2A PKC Δ1−10, or empty expression vector and cultured in DMEM without phosphate containing 1% calf serum and L-glutamine (cellgro, Mediatech, Inc.). After 48 h, cells were labeled by addition of 0.6 mCi/mL ^{32}P-orthophosphate (Perkin-Elmer) for 6 h, with or without 100 nM BIM or 50 ng/mL PMA. Duplicate transfections were performed without addition of labeled phosphate. Cell monolayers were washed with ice cold PBS and incubated with RIPA buffer (without deoxycholate) containing protease inhibitor cocktail and phosphatase inhibitor cocktail (Sigma Chemical Co.) at 4 °C for 10 min. Cells were harvested and lysed by passing through a 22 gauge needle, and cell debris was removed by centrifugation. The lysate was precleared with normal rabbit IgG antisera and Protein A/G Agarose (Santa Cruz). Lysate was incubated with PITX2 antisera for 2 h followed by addition of Protein A/G Agarose overnight at 4 °C. Beads were pelleted and proteins solubilized using SDS loading buffer, boiled and resolved on a 10% polyacrylamide gel. Gel was exposed to film to determine phosphorylation of proteins by incorporation of labeled phosphate. A Western blot was performed on duplicate immunoprecipitation samples that were not labeled to confirm protein expression.

RESULTS

Phosphorylation of PITX2A by Protein Kinase C. Analysis of the PITX2A protein revealed 10 consensus protein kinase C (PKC) sites located throughout the protein (Figure 1A). These are designated as PKC sites 1−10 starting at the N terminus of PITX2A; complete sites are PKC #1, residues 7−10 (Ser^{10}); PKC #2, residues 17−20 (Ser^{20}); PKC #3, residues 34−36 (Ser^{34}); PKC #4, residues 41−44 (Thr^{44}); PKC #5, residues 67−69 (Ser^{67}); PKC #6, residues 136−139 (Thr^{139}); PKC #7, residues 144−146 (Ser^{144}); PKC #8, residues 228−230 (Thr^{230}); PKC #9, residues 237−239 (Ser^{237}); and PKC #10, residues 255−258 (Ser^{258}). We asked if three serine/threonine kinases, PKC, CKII, and PKA, could phosphorylate PITX2A. PITX2A protein (0.5 μg) purified from bacteria as previously described (*15*) was incubated

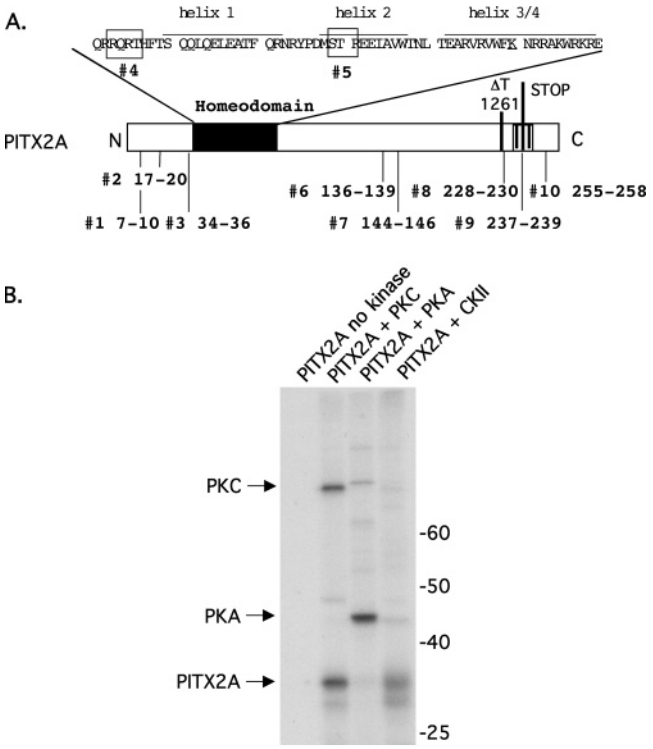

FIGURE 1: PITX2A phosphorylation by protein kinase C. (A) Schematic of the consensus PKC sites within the PITX2A homeodomain protein. Two sites are located in the homeodomain and are boxed out. The PKC consensus sites are shown within the protein by the amino acid numbers in bold. One site in the C terminus is located within the OAR domain; a 14 residue conserved region (striped box). The new C-terminal ARS mutation is shown where the T base is deleted at nucleotide 1261, which creates a stop codon within the OAR domain (striped box) of the PITX2A C-terminal tail. The lysine residue required for DNA binding in the third helix is underlined. (B) Identification of PKC as the serine/threonine kinase that phosphorylates PITX2A. Bacterial expressed and purified PITX2A (0.5 μg) was incubated with either casein kinase II (CKII), γ-^{32}P-ATP alone, protein kinase A (PKA), or protein kinase C (PKC) and analyzed on an SDS polyacrylamide gel. The gels were exposed to film for 30 min to obtain the autoradiographs. Molecular weight markers are indicated on the side.

with CKII, PKA, or PKC. Specific phosphorylation of PITX2A occurred with PKC and some residual phosphorylation by CKII and no phosphorylation of PITX2A by PKA (Figure 1B). There are two consensus CKII sites in PITX2A located at residues 34−31 and 66−69. These sites appear to be phosphorylated at low levels using pure CKII preparations (Figure 1B). As a control, the protein kinases used in these experiments were incubated with specific peptide substrates to demonstrate that each kinase was active. The neurogran peptide (10 ng), a substrate for PKC, kemptide peptide (10 ng), a substrate for PKA, and CKII peptide (10 ng), a substrate for CKII, were phosphorylated by their respective kinases (data not shown). Thus, the lack of PITX2A phosphorylation by PKA and reduced phosphorylation by CKII was not due to inactive kinase preparations. The specific activities of all kinases were calculated, and units were adjusted to ensure that equal amounts (specific activities transfer 10 pmol/min of phosphate) of the kinases were added to each reaction.

PITX2A Is Phosphorylated by Endogenous PKC. To determine if PITX2A was phosphorylated by endogenous PKC, nuclear extracts were prepared from GH3, LS-8, and

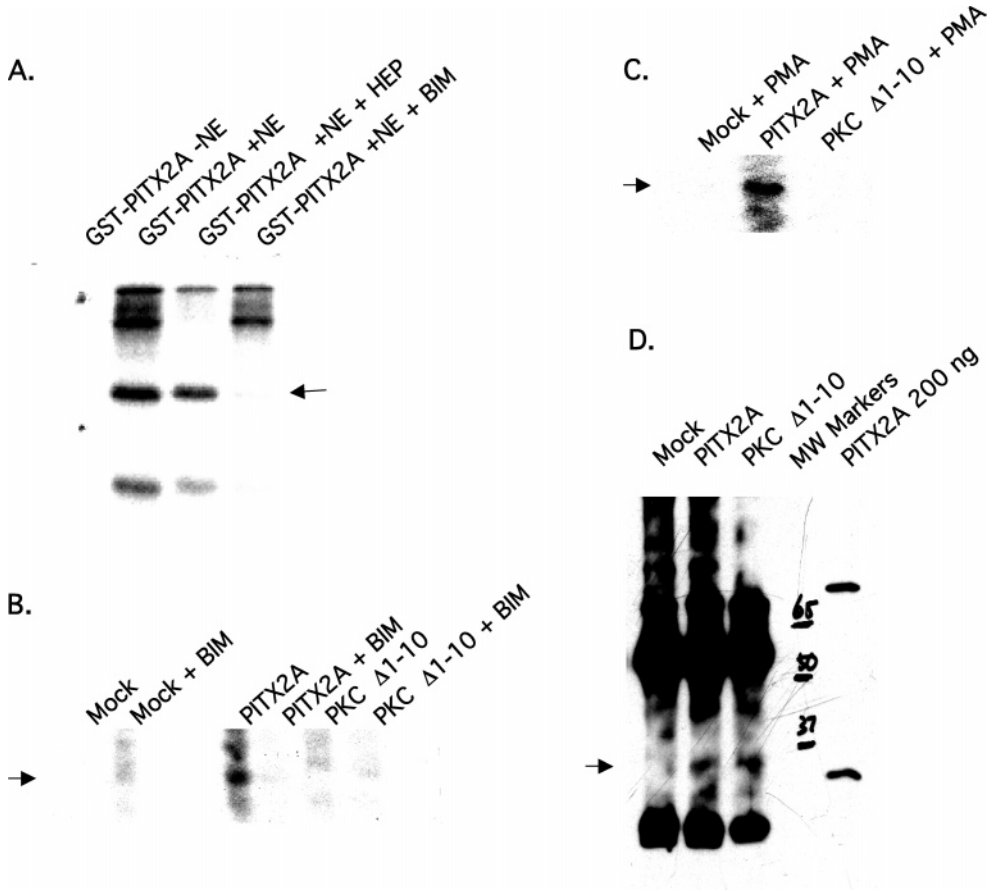

FIGURE 2: Endogenous PKC phosphorylates PITX2A. (A) GST-PITX2A was expressed in bacteria, purified, and immobilized on glutathione sepharose beads. Immobilized GST-PITX2A (~1 μg) was incubated with GH3 nuclear extract (NE), γ-^{32}P-ATP, and kinase buffer in the presence or absence of PKC inhibitors and the phosphorylated proteins resolved on a 10% SDS gel. As a control, GST-PITX2A was assayed in the presence of γ^{32}P-ATP but without NE. In the presence of NE the GST-PITX2A protein was efficiently phosphorylated and addition of heparin (HEP), a specific inhibitor of CKII, had no effect on PITX2A phosphorylation. However, addition of BIM, a specific inhibitor of PKC, inhibited PITX2A phosphorylation by the NE. The arrow points to the phosphorylated GST-PITX2A protein. All gels were stained with Coomassie blue to visualize the GST-PITX2A protein and confirm the corresponding phosphorylated band. (B) In vivo phosphorylation of PITX2A detected by immunoprecipitation of ^{32}P labeled PITX2A. CHO cells transfected with either PITX2A, PITX2A PKC Δ1−10, or empty expression vector were labeled with ^{32}P-orthophosphate and lysed and the expressed proteins immunoprecipitated using PITX2 affinity purified antisera. BIM was added to duplicate samples to specifically inhibit PKC activity. Immunoprecipitation of cells transfected with empty expression vector (mock) did not reveal a protein corresponding to the size of PITX2A. Labeled PITX2A was immunoprecipitated (arrow points to labeled PITX2) indicating that it was phosphorylated and the duplicate experiment in the presence of BIM inhibited PITX2 phosphorylation in the cell. The PITX2A PKC Δ1−10 mutant protein was not labeled. Immunoprecipitated samples were resolved on a 10% SDS gel and exposed to film to visualize the ^{32}P-labeled PITX2A protein. (C) CHO cells were transfected with PITX2 and the protein immunoprecipitated as in B; however, PMA was added to the cell cultures. (D) Immunoprecipitation of nonlabeled proteins expressed in transfected CHO cells. Duplicate transfections were performed as in B without addition of ^{32}P-orthophosphate. Cells were lysed, and immunoprecipitated proteins were detected by Western blot. PITX2A and PITX2A PKC Δ1−10 were expressed and immunoprecipitated demonstrating equal expression of both proteins. Purified PITX2A (200 ng) was run on the gel as a positive control.

CHO cells. The GH3 cell line represents a pituitary cell line, LS-8 was derived from mouse molar epithelium, and both have been shown to endogenously express PITX2 (*3*, *20*). GST-PITX2A fusion protein was immobilized to glutathione Sepharose beads and incubated with nuclear extracts under phosphorylation conditions; after incubation the beads were washed (4 times with kinase buffer) and protein was resolved on a polyacrylamide gel and exposed to film. PITX2A was phosphorylated by endogenous kinase activity from GH3 nuclear extracts (Figure 2A). Phosphorylation by endogenous PKC was also observed using LS-8 nuclear extracts and CHO nuclear extracts (data not shown). Heparin (Hep), which specifically inhibits CKII activity, and BIM, which inhibits PKC activity, were used to demonstrate that PKC was responsible for the endogenous kinase activity. Addition of heparin to the nuclear extracts did not inhibit PITX2A phosphorylation, indicating that endogenous CKII activity is not phosphorylating PITX2A. Therefore, the low level of CKII phosphorylation observed in Figure 1B using pure CKII appears to be an artifact. However, BIM addition inhibited over 90% of PITX2A phosphorylation by nuclear extracts, indicating specific phosphorylation by PKC (Figure 2A).

To demonstrate in vivo phosphorylation of PITX2A, CHO cells were transfected with PITX2A and PITX2A PKC Δ1−10, which has all 10 PKC sites mutated by changing serines or threonines to alanines or glycines. Cells were labeled by the addition of ^{32}P-orthophosphate and lysed, and protein was immunoprecipitated using PITX2 affinity purified antisera. PITX2A was phosphorylated and immunoprecipitated, and duplicate transfection experiments in the presence of BIM, a PKC inhibitor, inhibited endogenous PKC phosphorylation of PITX2A (Figure 2B). Furthermore, the specificity of PITX2A phosphorylation by PKC is shown through the absence of a labeled PITX2A PKC Δ1−10 immunoprecipi-

tated protein (Figure 2B). As a control, CHO cells were transfected with empty vector (mock) (Figure 2B).

A second immunoprecipitation experiment was performed to demonstrate that PKC stimulation by PMA did not phosphorylate the PITX2 PKC Δ1−10 mutant. Addition of PMA did not result in phosphorylation of the PKC Δ1−10 mutant protein (Figure 2C).

To control for transfection and immunoprecipitation efficency, duplicate unlabeled transfected CHO cells were immunoprecipitated using the PITX2 antibody and the expressed immunoprecipitated proteins were visualized by Western blot immunochemistry (Figure 2D). The Western blot is shown overexposed to reveal all bands in this blot. Therefore, the lack of PITX2A PKC Δ1−10 phosphorylation was not due to decreased expression in the transfected cells or defective immunoprecipitation.

Mutational Analysis of the Ten PITX2A PKC Sites. To demonstrate site specific PITX2A phosphorylation by PKC, specific mutations were made changing serine/threonine residues to alanines or glycines in the consensus PKC phosphorylation sites. Mutation of the first two (numbering starting at N terminus as 1) N-terminal PKC sites (PITX2A PKC Δ1−2) resulted in ∼20% reduction in phosphorylation compared to wild type, and subsequent mutation of the first 4 PKC sites (PITX2A PKC Δ1−4) resulted in a 60% decrease in PITX2A phosphorylation compared to wild type (Figure 3A,C). Mutation of the first five PKC sites in PITX2A PKC Δ1−5 protein resulted in a further decrease in phosphorylation compared to wild type (Figure 3A,C). When all PKC sites were mutated except for PKC site #5, Ser^{67} (PITX2A PKC Δ1−4, 6−10), a small amount of phosphorylation was observed due to the presence of the #5 PKC site (Figure 3A,C). As expected, mutation of the last 6 PKC sites (PITX2A PKC Δ5−10) resulted in 85% decreased phosphorylation compared to wild type (Figure 3A,C). A corresponding increase in PITX2A phosphorylation occurred when the last 5 (PITX2A PKC Δ6−10) or 3 PKC sites were mutated (PITX2A PKC Δ8−10), respectively, compared to PITX2A PKC Δ5−10 (Figure 3A,C). When all 10 PKC sites were mutated (PITX2A PKC Δ1−10), we observed a complete loss of phosphorylation by PKC (Figure 3A,C). A silver stained protein gel is shown to confirm relative protein concentrations of each protein used in the assays (Figure 3B). All protein preparations were quantitated and normalized to wild type (using image analysis programs) to ensure that equal amounts of proteins were used in all kinase assays.

In addition, purified PITX2A C-terminal, C-terminal truncated, and homeodomain peptides were prepared from bacteria and tested for phosphorylation by PKC. The complete C-terminal tail peptide (PITX2 C173, containing 6−10 PKC sites) and the last 78 and 39 amino acid peptides (PITX2 C78, containing 8−10 PKC sites and PITX2 C39, containing 9−10 PKC sites) were all rapidly phosphorylated by PKC. The homeodomain peptide was also phosphorylated by PKC (data not shown). The phosphorylation of several C-terminal truncated proteins were compared to wild-type PITX2A. Deletion of the last 39 (PKC 9−10 sites) and 78 (PKC 8−10 sites) residues resulted in a loss of phosphorylation compared to wild type (data not shown).

Phosphorylation of the C-terminal proteins, homeodomain peptide, and C-terminal truncated proteins (which contain the N-terminal PKC sites) (data not shown) further confirm

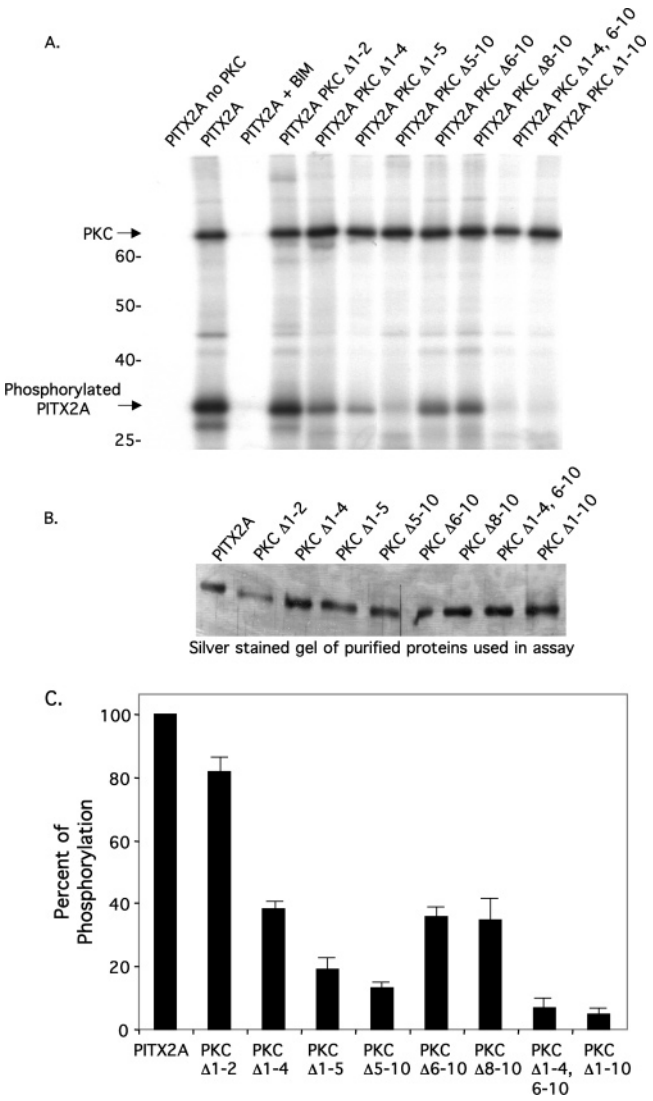

FIGURE 3: Mutational analysis of the ten PITX2 PKC sites. (A) PITX2A (0.5 μg) and PITX2A PKC site mutants (0.5 μg) were phosphorylated by PKC and resolved on an SDS gel. The numbering of the PKC sites begins at the N terminus with number 1. Specific serines or threonines were substituted with either an alanine or glycine (see text for complete details). (B) A silver stained gel of the PITX2A and PKC mutant proteins used in the assay. The stained gels were quantitated and all protein concentrations normalized to wild type to ensure that equal protein amounts were added to the kinase reactions. (C) Quantitation of the phosphorylated PITX2A PKC mutant proteins and comparison to the PITX2A phosphorylated protein. The percent activities vs PITX2A are shown (± SEM from three independent experiments).

that the PKC sites are functional and phosphorylated by PKC. While each individual PKC site was not assayed independently, the combination of specific mutations of two or more sites combined with our analysis of truncated and deleted PITX2A proteins revealed that the PKC sites within the N-terminus, homeodomain, and C-terminus are phosphorylated. Furthermore, while conservative mutations were made, we cannot rule out that these mutations may impart a conformational change in the protein. These effects could result in differential phosphorylation of specific residues when several sites are mutated. This may explain small differences in phosphorylation observed between different sets of mutants.

PITX2A PKC Mutant Proteins Retain Their DNA Binding Activity. In order to analyze the PITX2A PKC mutants in

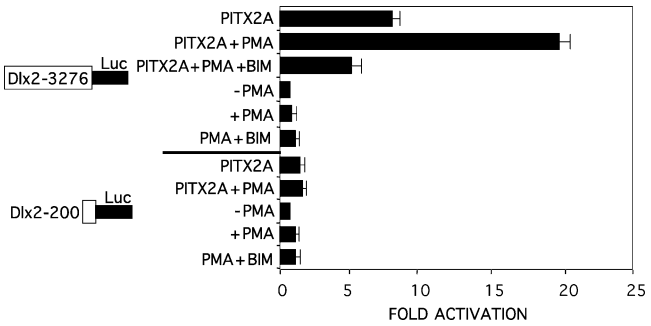

FIGURE 4: PKC stimulation increases transcriptional activation by PITX2A. CHO cells were transfected with 5 μg of either the Dlx2-3276 or Dlx2-200 luciferase reporter genes. The cells were cotransfected with 2.5 μg of either the *CMV-PITX2* or the CMV plasmid without *PITX2* (vector control). CHO cell lysates transfected with empty vector were used as a control to demonstrate lack of endogenous PITX2 protein in CHO cells. PMA (50 ng/mL) and BIM (100 nM) were added immediately after transfection, and 24 h later cells were harvested and assayed for luciferase and β-galactosidase activities. As a control BIM and PMA were added to cells transfected with the reporter plasmids and empty expression vector. To control for transfection efficiency, all transfections included the CMV β-galactosidase reporter. Cells were incubated for 24 h and then assayed for luciferase and β-galactosidase activities. The activities are shown as mean fold activation compared to the *Dlx2* promoter plasmids without *PITX2* expression and normalized to β-galactosidase activity ($\pm$ SEM from six independent experiments). The mean *Dlx2* promoter luciferase activity with PITX2 expression was approximately 80000 light units per 15 μg of protein, and the β-galactosidase activity was about 70000 light units per 15 μg of protein.

transfection assays, it was essential to determine their DNA binding properties. All PKC mutant proteins (80 ng) bound DNA similarly to wild type (data not shown).

PKC Stimulation Increased PITX2A Transcriptional Activity. The activities of the minimal *Dlx2* promoter (Dlx2-200-luc), which contains only the TAATAA box and 200 bp of 5′ flanking sequences, were compared to the activities of the full-length promoter (Dlx2-3276-luc) containing upstream regulatory elements. Transfection of CHO cells with Dlx2-3276-luc and PITX2A resulted in 8-fold activation of this full-length promoter (Figure 4). As a control, PITX2A minimally activated the minimal Dlx2-200-luc promoter (Figure 4).

Addition of PMA (a phorbol ester and specific stimulator of PKC activity) to PITX2A transfected CHO cells increased the activation of the Dlx2-3276-luc reporter from 8-fold to ~20-fold (Figure 4). PMA alone (without PITX2A expression) did not activate the Dlx2-3276-luc promoter compared to controls without PMA (Figure 4). These data demonstrate the specificity of PMA in activating only PITX2A activity and not a nonspecific effect on the *Dlx2* promoter. The minimal Dlx2-200-luc reporter was not further activated in the presence of PITX2A and addition of PMA (Figure 4). PMA alone had no effect on activation of the minimal *Dlx2* promoter (Figure 4). Furthermore, the concentration of PMA used in these experiments does not have a generalized effect on transcription and is specific for PITX2A transcriptional activation.

To address the specificity of PKC stimulated phosphorylation and transcriptional activity of PITX2A by PMA, BIM (100 nM) was added to PITX2A transfected CHO cells prior to addition of PMA. BIM completely inhibited the transcriptional activity of PITX2A stimulated by PMA (Figure 4). Furthermore, BIM treatment had no effect on CHO cells transfected with Dlx2-200-luc (Figure 4). Additionally, PKI, a peptide PKC inhibitor, was used, and we received similar results (data not shown).

Western blot analysis was performed using 10 μg of transfected cell lysates to demonstrate expression of PITX2A protein (data not shown). We have previously shown PITX2A protein expression in transfected CHO cells (*20*).

Dlx2 Expression Is Down Regulated in the Pitx2 Mutant Mouse. We have previously reported that PITX2 specifically activates the *Dlx2* promoter (*20*, *24*). However, to demonstrate in vivo regulation of *Dlx2* expression by *Pitx2*, we performed expression profiling studies on *Pitx2* mutant mouse tissues. *Dlx2* is expressed in the dental epithelium and craniofacial region of mouse embryos (*52*−*55*). *Pitx2* and *Dlx2* are coexpressed in the dental epithelium during tooth development, and we isolated face tissue containing the dental epithelium to determine levels of *Dlx2* transcripts. Analysis of *Pitx2*$^{-/-}$ mutant mice reveal for the first time decreased *Dlx2* transcripts from E14.5 face tissue compared to wild-type embryos. Total RNA was extracted and used to detect *Dlx2* and *β-actin* gene expression. RT-PCR experiments demonstrate a reduction in *Dlx2* expression from the *Pitx2* mutant mice (Figure 5A). To more definitively demonstrate reduced *Dlx2* expression in the *Pitx2* mutant mice, quantitative RT-PCR experiments were performed using total RNA isolated from the face tissues. Comparison of the Ct values between wild-type and mutant mice revealed a 2.3-fold decrease in *Dlx2* transcripts in the mutant mice (Figure 5B). Samples were analyzed from 3 separate mice and 3 separate RNA samples, and *Dlx2* transcripts were normalized to β-actin transcripts to control for RNA preparations. Melting curves were analyzed for each experiment to ensure that specific products were produced. These data reveal a potential link between *Pitx2* and *Dlx2* expression.

N-Terminal and C-Terminal Phosphorylation Modulates PITX2A Transcriptional Activity. Because a functional basis for the N terminus of PITX2A has not been identified, we asked if N-terminal phosphorylation affected PITX2A activity. CHO cells were cotransfected with the Dlx2-3276-luc promoter and PITX2A PKC mutations to determine their effect on transactivation. PITX2A PKC Δ1−2 (11-fold activation) and PITX2A PKC Δ1−4 (16-fold activation) demonstrate increased transcriptional activation of the *Dlx2* promoter compared to wild type (Figure 6A). N-Terminal phosphorylation appears to inhibit PITX2A transcriptional activity, since mutation of these sites results in increased activity.

The role of C-terminal phosphorylation is revealed by specific mutations of the C-terminal tail PKC sites. PITX2A PKC Δ6−10 (4-fold activation) and PITX2A PKC Δ8−10 (5-fold activation) demonstrated decreased activity, compared to wild type (Figure 6A). These C-terminal PKC mutations reveal that phosphorylation of the PITX2A C-terminal tail is required for maximal transcriptional activity. These data reveal differences in the activities of the N-terminal and C-terminal regions through phosphorylation events. As expected, mutation of all ten PKC sites (PITX2A PKC Δ1−10) resulted in decreased PITX2A transcriptional activity at 4-fold compared to 8-fold for wild type (Figure 6A).

Transfected CHO cell lysates were assayed for PITX2A PKC mutant expression by Western blot analysis to dem-

A.

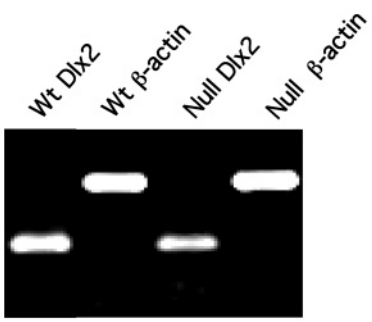

B.

Relative Abundance of *Dlx2* transcripts normalized to *β-actin* transcripts	
***Pitx2* null mutant mouse face tissue compared to wildtype**	***Dlx2***
$E^{\Delta\Delta CT}$ (expressed as fold reduction) N=3	R*= 0.44 **2.3 +/- 0.06**

FIGURE 5: *Dlx2* expression is down regulated in *Pitx2*$^{-/-}$ homozygous mice. (A) Total RNA was isolated from E14.5 wild-type and Pitx2$^{-/-}$ mouse facial tissue containing nasal, maxillary, and mandibular prominences. RT-PCR was performed with 1 μg of RNA from both mice using *Dlx2* and *β-actin* specific primers. *Dlx2* expression is reduced in the mutant mouse tissue. All bands were sequenced to confirm their identity. (B) Quantitative RT-PCR demonstrates a specific decrease in *Dlx2* transcripts in the mutant mouse. Real-time RT-PCR was performed with 2 μg of RNA and the same primers as in A, and melting curves were analyzed after each run to ensure the quality of the product. Total RNA was analyzed from 3 separate mice (both wild type and mutant), and Ct values were calculated and *Dlx2* transcript levels normalized to *β-actin*. The normalized differences in Ct values are expressed as fold reduction (*51*).

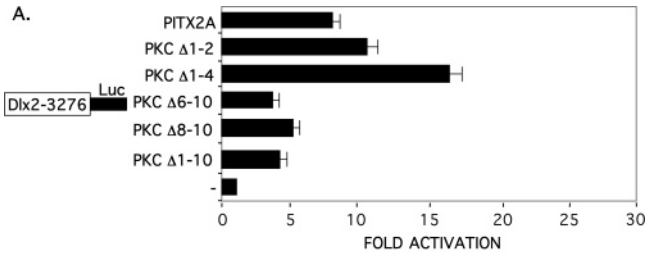

FIGURE 6: Phosphorylation modulates the N- and C-terminal transcriptional activity of PITX2A. (A) CHO cells were transfected as described in Figure 4. The activities are shown as mean fold activation compared to the *Dlx2* promoter plasmid without *PITX2* expression and normalized to β-galactosidase activity ($\pm$ SEM from six independent experiments). (B) Western blot of transfected CHO cell lysates (10 μg) using the PITX2 (P2R10) antibody and ECL reagents from Amersham.

onstrate that differences in transcriptional activities were not due to unequal expression or protein degradation in these cells (Figure 6B). All mutant proteins are equally expressed and are not degraded as shown in Figure 6B.

PKC Stimulation Activates PITX2A N-Terminal PKC Mutants but not C-Terminal PKC Mutants. We next asked if stimulated N-terminal and/or C-terminal PITX2 phosphorylation affected its activity. PMA induced PKC activity in transfected CHO cells increased PITX2A transcriptional activation of the *Dlx2* promoter from 8-fold to 20-fold (Figure 7). The PITX2A PKC Δ1−4 mutant is further stimulated by PMA addition to transfected CHO cells from 16-fold to 27-fold activation of the *Dlx2* promoter (Figure 7). Therefore, decreased phosphorylation of the PITX2A N-terminal sites results in an increase in transcriptional activity and/or increased C-terminal phosphorylation stimulated PITX2 activity. PMA addition did not increase the transcriptional activity of the PITX2A PKC Δ6−10 or the PKC Δ8−10 mutant, which may suggest that N-terminal phosphorylation is inhibitory to PITX2A activity (Figure 7). Thus, phosphorylation of the C-terminal tail enhances transcriptional activation and N-terminal phosphorylation is inhibitory to PITX2A activity. PMA addition had no effect on the PITX2A PKC Δ1−10 mutant as expected (Figure 7).

PITX2A C-Terminal Phosphorylation Facilitates Protein Interactions. To provide a functional mechanism for PITX2A phosphorylation by PKC, we asked if phosphorylation affected its interaction with the pituitary POU homeodomain protein, Pit-1. We have previously shown a direct interaction between Pit-1 and the PITX2 C-terminal tail (*18*). Cotransfection of CHO cells with the *prolactin* promoter and PITX2A demonstrate a 6-fold activation of this promoter (Figure 8). Pit-1 activates the *prolactin* promoter at 4-fold, and cotransfection of PITX2A and Pit-1 yielded a 38-fold synergistic activation of the *prolactin* promoter (Figure 8). Therefore, to determine if phosphorylation of the PITX2A C-terminal tail was required for this synergistic activation, Pit-1 was cotransfected with the PITX2A PKC mutations. PITX2A PKC Δ1−10 transactivates the *prolactin* promoter at only 2-fold, or a 3-fold decrease compared to wild type (Figure 8). Cotransfection of Pit-1 with PITX2A PKC Δ1−10 did not result in synergism, only additive activation of $<$10-fold (Figure 8). The PITX2A C-terminal PKC mutants, PITX2A PKC Δ6−10 and Δ8−10, yielded decreased activation of the *prolactin* promoter compared to wild type (3-fold activation), and cotransfection with Pit-1 did not result in synergistic activation of the *prolactin* promoter by either PKC C-terminal mutant (15-fold activation) (Figure 8). However, the N-terminal PKC mutant, PITX2A PKC Δ1−4, increased the activation of the *prolactin* promoter compared to wild type at 15-fold (Figure 8). PITX2A PKC Δ1−4 cotransfection with Pit-1 yielded a synergistic activation at 38-fold, similar to wild type (Figure 8). These data indicate that PITX2 C-terminal phosphorylation enhances Pit-1 interaction and synergistic activation of the *prolactin* promoter.

Reduced Phosphorylation of a PITX2 C-Terminal ARS Mutation. A new C-terminal PITX2A mutation associated with ARS results in the deletion of a T nucleotide at position 1261 of PITX2A (Figure 1A). Deletion of this T creates a new reading frame change in the 3′ end of the C-terminal tail. Starting at residue 226, the reading frame is changed and a premature stop codon is created 12 codons downstream

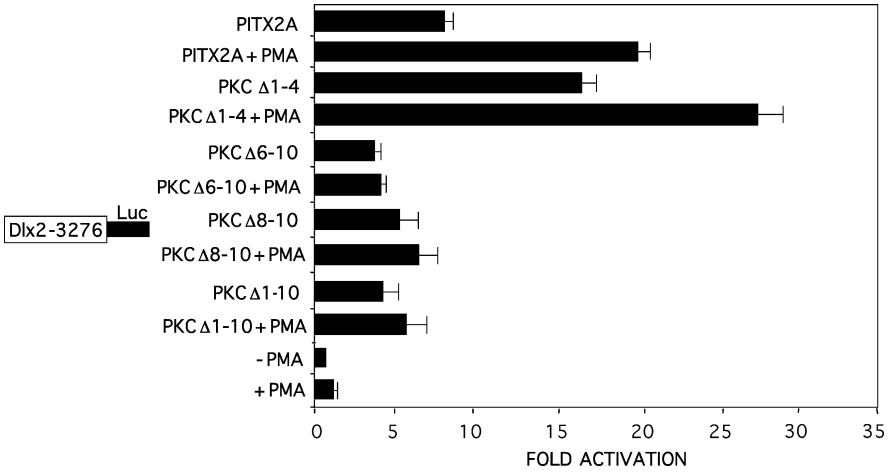

FIGURE 7: PMA stimulated phosphorylation differentially regulates PITX2A PKC mutant transcriptional activities. CHO cells were transfected as in Figure 4 with and without PMA (50 ng/mL) addition. The activities are shown as mean fold activation compared to the *Dlx2* promoter plasmid without *PITX2* expression (± PMA addition) and normalized to β-galactosidase activity (± SEM from five independent experiments).

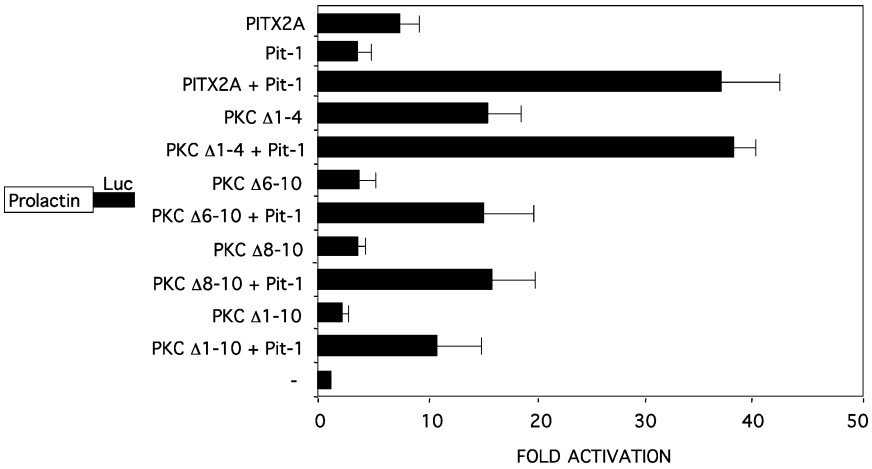

FIGURE 8: PITX2A C-terminal phosphorylation facilitates transcriptional synergy with the Pit-1 homeodomain protein. CHO cells were transfected with the prolactin 2.5-luciferase reporter plasmid and cotransfected with PITX2A, PITX2A PKC mutations, or the parental CMV expression plasmid without PITX2A (−) with and without 2.5 μg of Pit-1 (*18*). All transfection assays were performed as described in Figure 4. The activities are shown as mean fold activation compared with the prolactin promoter plasmid without PITX2A or Pit-1 expression and normalized to β-galactosidase activity (± SE from four independent experiments).

(Figure 1A). Thus, this mutant protein (PITX2A ΔT1261) is only 237 amino acids compared to 271 for PITX2A and completely disrupts the PITX2A C-terminal OAR domain. This mutation removes 3 PKC sites and results in decreased phosphorylation compared to wild type (Figure 9). This would be expected and is similar to PITX2A PKC Δ8−10 phosphorylation.

Impaired Transcriptional Activation by the ARS PITX2A Mutant. We asked if the new ARS mutation would affect DNA binding activity. The C-terminal PITX2A ΔT1261 mutant protein bound DNA similarly to wild-type protein (Figure 10A). Transfection of the PITX2A ΔT1261 mutation revealed a 2-fold decrease in activation of the *Dlx2* promoter compared to wild type (4-fold activation compared to 8-fold activation, respectively) (Figure 10B). Furthermore, this mutant was not stimulated by addition of PMA to transfected cells (Figure 10B). Thus, deletion of the C-terminal PKC sites and the corresponding residues removes its ability to be activated by PKC phosphorylation. This naturally occurring PITX2 mutation corroborates the data from the PITX2A PKC Δ8−10 mutant. The PITX2A ΔT1261 mutation disrupts the OAR domain, which may adversely affect transcriptional activation by PITX2, independent of phospho-

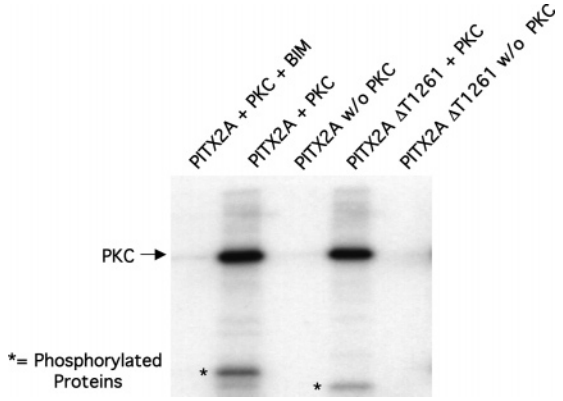

FIGURE 9: Reduced phosphorylation of the PITX2A ΔT1261 mutant protein. PITX2 and PITX2A ΔT1261 proteins were expressed in bacteria, isolated, and phosphorylated by PKC. Phosphorylated proteins (0.5 μg) were resolved on a 12.5% SDS polyacrylamide gel and analyzed by autoradiography and phosphorimaging. The autophosphorylated PKC subunit is indicated at the top of the gel, and asterisks at the bottom of the gel indicate the smaller phosphorylated PITX2 proteins. All protein preparations were quantitated and normalized to wild type (using image analysis programs) to ensure that equal amounts of proteins were used in all kinase assays.

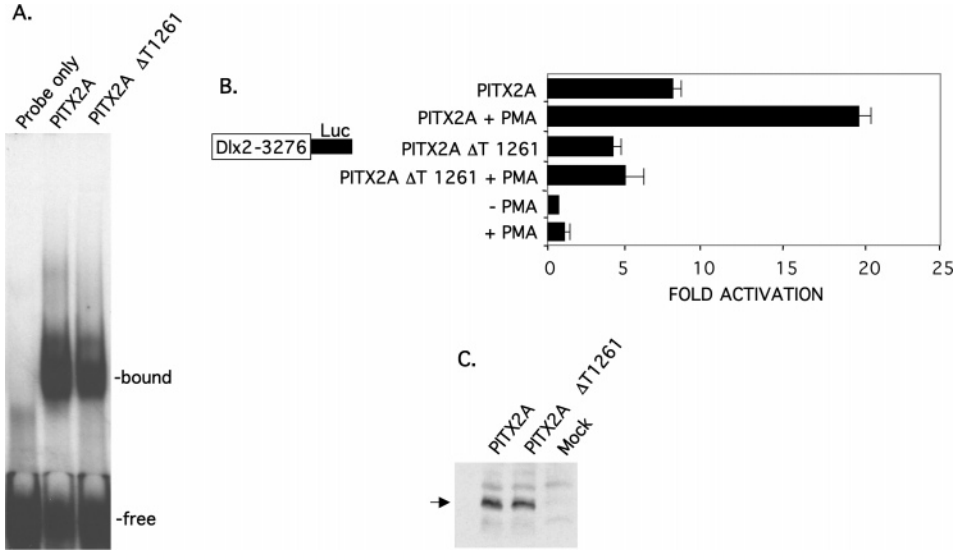

FIGURE 10: PKC stimulation does not increase the transcriptional activity of the ARS PITX2A ΔT1261 protein. (A) EMSA of PITX2A and ARS PITX2A mutant protein (80 ng) incubated with the *Dlx2 bicoid* sequence (5′TAATCC3′) as the radioactive probe. The location of bound and free probe is indicated. (B) CHO cells were transfected as previously described, with and without PMA addition (*56*). The activities are shown as mean fold activation compared to the *Dlx2* promoter plasmid without *PITX2* expression (± PMA) and normalized to β-galactosidase activity (± SEM from four independent experiments). (C) Protein expression was confirmed by Western blot analysis of transfected cell lysates.

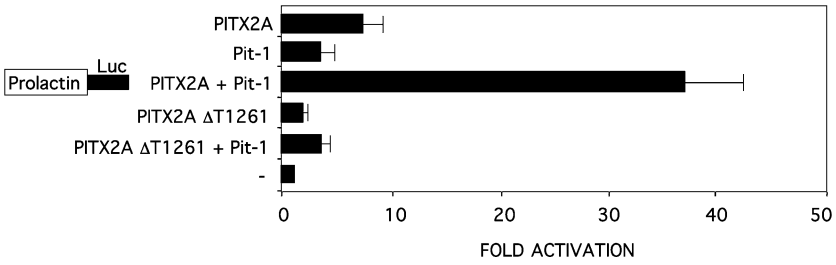

FIGURE 11: PITX2A ΔT1261 cannot synergize with the Pit-1 homeodomain protein. CHO cells were transfected with the prolactin 2.5-luciferase reporter plasmid and cotransfected with PITX2A, PITX2A ΔT1261 mutation, or the parental CMV expression plasmid without PITX2A (−) with and without 2.5 μg of Pit-1 (*18*). All transfection assays were performed as previously described (*56*). The activities are shown as mean fold activation compared with the prolactin promoter plasmid without PITX2A or Pit-1 expression and normalized to β-galactosidase activity (± SE from four independent experiments).

rylation. Further experiments are required to differentiate the effects of C-terminal phosphorylation and the OAR domain in regulating PITX2 activity. However, this mutation does provide a new mechanism for the developmental defects in ARS patients through a C-terminal mutation that affects phosphorylation and reduces PITX2 activity.

Transfected CHO cell lysates were assayed for PITX2A and PITX2A mutant expression by Western blot analysis to demonstrate that differences in transcriptional activities were not due to unequal expression or protein degradation in these cells (Figure 10C).

Disrupted PITX2 Protein Interactions as a Molecular Basis for ARS. To provide a functional mechanism for the *PITX2A ΔT1261* mutation, we asked if it affected the interaction with the pituitary POU homeodomain protein, Pit-1. As shown previously, Pit-1 activates the *prolactin* promoter at 4-fold, and cotransfection of PITX2A and Pit-1 yielded a 38-fold synergistic activation of the *prolactin* promoter in CHO cells (Figure 11). *PITX2A ΔT1261* was unable to interact with Pit-1 to synergistically activate the *prolactin* promoter (Figure 11). This mutation provides a functional analysis of PITX2 phosphorylation and protein interactions in regulating normal human development. Furthermore, these data corroborate a role for the PITX2 C-terminal tail in regulating protein interactions (*18*).

DISCUSSION

Protein Kinase C Phosphorylates PITX2. It has previously been shown that protein interactions can occur through the C-terminal tail of PITX2. Phosphorylation of PITX2 facilitates dimer formation and suggests that dimers may enhance transcriptional activation (*56*). Thus, PITX2 dimerization appears important for transactivation. We are investigating the posttranscriptional modulation of PITX2, and in this report we provide a functional mechanism for the role of phosphorylation in regulating these interactions. Phosphorylation of proteins can promote dimer formation, which may be a mechanism for increasing transcription activity. It has been shown that phosphorylation of the Nkx2.5 homeodomain protein by casein kinase II increases DNA binding and facilitates the formation of homodimers (*57*). PITX2 isoforms can form heterodimers to synergistically regulate gene expression (*24*). PITX2A PKC site mutations specifically demonstrate phosphorylation by PKC. PITX2 phosphorylation was demonstrated using nuclear extracts, immunoprecipitation experiments, and treatment of transfected cells with specific PKC inhibitors. The functional signifi-

cance of PITX2 phosphorylation was shown through specific PITX2 PKC mutants, a naturally occurring PITX2 ARS mutant, and interaction of a protein known to bind the PITX2 C-terminal tail (*18*). PITX2 phosphorylation appears to play a role in regulating the interaction and dimer formation between PITX2 isoforms.

The three major PITX2 isoforms (A, B, and C) contain dissimilar N-terminal domains (*24*, *29*). The role of these different N termini has not yet been determined; however, these data suggest that N-terminal phosphorylation may inhibit PITX2A transcriptional activity. We have reported differences in PITX2 isoform transcriptional activities that are cell dependent, which would indicate that factors differentially interact with the N termini of each isoform (*24*). PITX2A and PITX2C activate the *Dlx2* promoter, while PITX2B is inactive conversely; PITX2B activates the *prolactin* promoter at higher levels than PITX2A or PITX2C (*24*). The N-terminal regions of each isoform contain different PKC sites; PITX2A has 3, PITX2B has 5, and PITX2C has 3. We speculate that increased phosphorylation of the PITX2B isoform may reduce its activity, as reported with the *Dlx2* promoter. This mechanism would seem likely since phosphorylation of the PITX2A N-terminus inhibits its activity. Furthermore, the reduced transcriptional activity of the C-terminal PKC mutants (PITX2A PKC Δ6−10 and PKC Δ8−10) may be due to N-terminal phosphorylation inhibiting their activity. However, PITX2B activation of the *prolactin* promoter may indicate a mechanism where N-terminal phosphorylation could activate its transcriptional activity in a promoter dependent fashion. Because PKC isoforms are tissue specific and levels of their expression vary in these tissues, this could provide a mechanism for the different PITX2 isoform transcriptional activities observed in multiple cell lines and with different promoter constructs.

The stoichiometry of PITX2 phosphorylation has not been determined, and in this report we make no claims to the regulation of PITX2 phosphorylation through mechanisms of cooperative phosphorylation. Phosphorylation of one site might influence phosphorylation at other sites, and mutation of specific PKC sites could affect phosphorylation at other sites.

PITX2 C-Terminal Phosphorylation Facilitates Protein Interactions and Transcriptional Activity. We have shown that PITX2 C-terminal phosphorylation regulates the synergistic activation of *prolactin* expression in concert with Pit-1. A model was proposed where Pit-1 binding to the PITX2 C-terminal tail opened up the C-terminal tail and relieved the inhibitory effect of its interaction with the N terminus (*18*). This model has been validated by several laboratories that have also reported the inhibitory nature of the PITX2 C-terminal tail (*22*, *58*). Addition of phosphates to the PITX2A protein would change its conformation and presumably allow for increased protein interactions. The model suggests that intramolecular folding of the full-length PITX2 protein brings the C-terminal tail in direct contact with the N-terminal domain (*18*). This folding interferes with DNA binding by the homeodomain. However, addition of phosphate groups to PITX2 may relieve this intramolecular folding and interaction of the C-terminal tail with the N terminus. In support of this we have shown that PITX2 phosphorylation increases DNA binding and transcriptional activity (ref *56* and this report). N-Terminal phosphorylation decreases transcriptional activity, and C-terminal tail phosphorylation increases PITX2A transcriptional activity through mechanisms that may involve intramolecular folding and/or protein interactions. Pit-1 binding to PITX2 may result in a conformational change of the C-terminal tail that unmasks the homeodomain and a potential transactivation domain (*18*). In the wild-type PITX2 protein, phosphorylation of the C-terminal tail presumably allows for factor interactions and increased transcriptional activity. We demonstrate a role for PITX2 phosphorylation and synergistic activation of *prolactin* in concert with Pit-1. PKC phosphorylation of the PITX2 C-terminal tail appears to facilitate a Pit-1 interaction and results in increased DNA binding activity and synergistic transcriptional activity.

Pit-1 phosphorylation regulates protein interactions as has been reported for its interaction with the ETS-1 protein (*59*). A Pit-1/ETS-1 interaction can synergistically activate the *prolactin* promoter (*60*). Pit-1 phosphorylation may affect its interaction with PITX2, and while the Pit-1 homeodomain was identified as an interaction site for ETS-1, the region that interacts with PITX2 is unknown.

To further demonstrate that the PITX2 C-terminal tail regulates its transcriptional activity, we tested a naturally occurring PITX2 C-terminal mutation associated with ARS. This mutation defines a role for PITX2 protein interactions in regulating normal human development. This is the most distal C-terminal mutation reported and results in a small deletion of the PITX2 C-terminal tail, including the OAR domain. This mutation corroborates our earlier studies demonstrating a role for this part of the PITX2 C-terminal tail in modulating its activity through a direct interaction with Pit-1 (*18*). PITX2 transcriptional regulation may be controlled through a similar mechanism involving other cellular proteins during development.

PKC plays a major role in tooth development and is expressed throughout tooth morphogenesis (*61*). However, a role for PKC in regulating transcription factors and gene expression during tooth development has not been shown. Genetic and epigenetic studies have shown that *Pitx2* is required for tooth development and is expressed at the earliest stages of tooth development (*12*, *13*, *48*, *62*, *63*). Furthermore, ARS patients with *PITX2* mutations present clinically with dental anomalies (*1*, *29*). In this report we have shown that PKC phosphorylation of PITX2 increases *Dlx2* expression. This would provide a mechanism to control the temporal and spatial expression of *Dlx2* during tooth development. In support of this model we are profiling gene expression in *Pitx2*$^{-/-}$ homozygous mice and demonstrate the reduction of *Dlx* expression in face tissue from these mice. The face tissue contains the maxillary and mandibular prominences which coexpress *Pitx2* and *Dlx2* at E14.5. These combined results suggest a potential role for PKC in regulating *Dlx2* expression through the phosphorylation of PITX2.

Previous studies on PKC have identified twelve different isomers, which share a similar catalytic domain but differ in their regulatory domains (*64*−*67*). The expression of these PKC isoforms is often tissue as well as differentiation stage specific (*68*). The identity of the PKC isomer involved in the modulation of PITX2 activity remains to be investigated. Because PITX2 is expressed throughout embryonic develop-

ment in several tissues, the regulated phosphorylation of PITX2 represents an important control point in its activation of target genes. PITX2 phosphorylation provides a mechanism for regulating the spatial and temporal expression of select genes during development.

ACKNOWLEDGMENT

We thank Lesley Kaufman for excellent technical assistance and Dr. Tord A. Hjalt (University of Lund, Lund, Sweden) for reagents and helpful discussions.

REFERENCES

1. Semina, E. V., Reiter, R., Leysens, N. J., Alward, L. M., Small, K. W., Datson, N. A., Siegel-Bartelt, J., Bierke-Nelson, D., Bitoun, P., Zabel, B. U., Carey, J. C., and Murray, J. C. (1996) Cloning and characterization of a novel bicoid-related homeobox transcription factor gene, RIEG, involved in Rieger syndrome, *Nat. Genet. 14*, 392−399.
2. Mucchielli, M., Martinez, S., Pattyn, A., Goridis, C., and Brunet, J. (1996) Otlx2, an Otx-Related Homeobox Gene Expressed in the Pituitary Gland and in a Restricted Pattern in the Forebrain, *Mol. Cell. Neurosci. 8*, 258−271.
3. Gage, P. J., and Camper, S. A. (1997) Pituitary homeobox 2, a novel member of the bicoid-related family of homeobox genes, is a potential regulator of anterior structure formation, *Hum. Mol. Genet. 6*, 457−464.
4. Campione, M., Steinbeisser, H., Schweickert, A., Deissler, K., van Bebber, F., Lowe, L. A., Nowotschin, S., Viebahn, C., Haffter, P., and Kuehn, M. R., Blum, M. (1999) The homeobox gene *Pitx2*: mediator of asymmetric left-right signaling in vertebrate heart and gut looping, *Development 126*, 1225−1234.
5. Yoshioka, H., Meno, C., Koshiba, K., Sugihara, M., Itoh, H., Ishimaru, Y., Inoue, T., Ohuchi, H., Semina, E. V., Murray, J. C., Hamada, H., and Noji, S. (1998) *Pitx2*, a Bicoid-Type Homeobox Gene, Is Involved in a Lefty-Signaling Pathway in Determination of Left-Right Asymmetry, *Cell 94*, 299−305.
6. Semina, E. V., Reiter, R. S., and Murray, J. C. (1997) Isolation of a new homeobox gene belonging to the Pitx/Rieg family: expression during lens development and mapping to the aphakia region on mouse chromosome 19, *Hum. Mol. Genet. 6*, 2109−2116.
7. Logan, M., Pagan-Westphal, S. M., Smith, D. M., Paganessi, L., and Tabin, C. J. (1998) The Transcription Factor Pitx2 Mediates Situs-Specific Morphogenesis in Response to Left-Right Asymmetric Signals, *Cell 94*, 307−317.
8. Piedra, M. E., Icardo, J. M., Albajar, M., Rodriguez-Rey, J. C., and Ros, M. A. (1998) *Pitx2* Participates in the Late Phase of the Pathway Controlling Left-Right Asymmetry, *Cell 94*, 319−324.
9. Ryan, A. K., Blumberg, B., Rodriguez-Esteban, C., Yonei-Tamura, S., Tamura, K., Tsukui, T., de la Pena, J., Sabbagh, W., Greenwald, J., Choe, S., Norris, D. P., Robertson, E. J., Evans, R. M., Rosenfeld, M. G., and Belmonte, J. C. I. (1998) Pitx2 determines left-right asymmetry of internal organs in vertebrates, *Nature 394*, 545−551.
10. St.Amand, T. R., Ra, J., Zhang, Y., Hu, Y., Baber, S. I., Qiu, M., and Chen, Y. P. (1998) Cloning and Expression Pattern of Chicken *Pitx2*: A New Component in the SHH Signaling Pathway Controlling Embryonic Heart Looping, *Biochem. Biophys. Res. Commun. 247*, 100−105.
11. Gage, P. J., Suh, H., and Camper, S. A. (1999) Dosage requirement of Pitx2 for development of multiple organs, *Development 126*, 4643−4651.
12. Lu, M., Pressman, C., Dyer, R., Johnson, R. L., and Martin, J. F. (1999) Function of Rieger syndrome gene in left-right asymmetry and craniofacial development, *Nature 401*, 276−278.
13. Lin, C. R., Kioussi, C., O'Connell, S., Briata, P., Szeto, D., Liu, F., Izpisua-Belmonte, J. C., and Rosenfeld, M. G. (1999) Pitx2 regulates lung asymmetry, cardiac positioning and pituitary and tooth morphogenesis, *Nature 401*, 279−282.
14. Szeto, D. P., Ryan, A. K., O'Connell, S. M., and Rosenfeld, M. G. (1996) P-OTX: A PIT-1-interacting homeodomain factor expressed during anterior pituitary gland development, *Proc. Natl. Acad. Sci. U.S.A. 93*, 7706−7710.
15. Amendt, B. A., Sutherland, L. B., Semina, E., and Russo, A. F. (1998) The Molecular Basis of Rieger Syndrome: Analysis of Pitx2 Homeodomain Protein Activities, *J. Biol. Chem. 273*, 20066−20072.
16. Tremblay, J. J., Lanctot, C., and Drouin, J. (1998) The pan-Pituitary Activator of Transcription, Ptx1 (Pituitary Homeobox 1), Acts in Synergy with SF-1 and Pit1 and Is an Upstream Regulator of the Lim-Homeodomain Gene Lim3/Lhx3, *Mol. Endocrinol. 12*, 428−441.
17. Tremblay, J. J., and Drouin, J. (1999) Egr-1 is a downstream effector of GnRH and synergizes by direct interaction with Ptx1 and Sf-1 to enhance luteinizing hormone beta gene transcription, *Mol. Cell. Biol. 19*, 2567−2576.
18. Amendt, B. A., Sutherland, L. B., and Russo, A. F. (1999) Multifunctional Role of the Pitx2 Homeodomain Protein C-Terminal Tail, *Mol. Cell. Biol. 19*, 7001−7010.
19. Hjalt, T. A., Semina, E. V., Amendt, B. A., and Murray, J. C. (2000) The Pitx2 Protein in Mouse Development, *Dev. Dyn. 218*, 195−200.
20. Green, P. D., Hjalt, T. A., Kirk, D. E., Sutherland, L. B., Thomas, B. L., Sharpe, P. T., Snead, M. L., Murray, J. C., Russo, A. F., and Amendt, B. A. (2001) Antagonistic Regulation of Dlx2 Expression by PITX2 and Msx2: Implications for Tooth Development, *Gene Expression 9*, 265−281.
21. Quirk, C. C., Lozada, K. L., Keri, R. A., and Nilson, J. H. (2001) A Single Pitx1 Binding Site Is Essential for Activity of the LH-(beta) Promoter in Transgenic Mice, *Mol. Endocrinol. 15*, 734−746.
22. Kioussi, C., Briata, P., Baek, S. H., Rose, D. W., Hamblet, N. S., Herman, T., Ohgi, K. A., Lin, C., Gleiberman, A., Wang, J., Brault, V., Ruiz-Lozano, P., Nguyen, H. D., Kemler, R., Glass, C. K., Wynshaw-Boris, A., and Rosenfeld, M. G. (2002) Identification of a Wnt/Dvl/β-catenin-Pitx2 Pathway Mediating Cell-Type-Specific Proliferation during Development, *Cell 111*, 673−685.
23. Ganga, M., Espinoza, H. M., Cox, C. J., Morton, L., Hjalt, T. A., Lee, Y., and Amendt, B. A. (2003) PITX2 Isoform-specific Regulation of Atrial Natriuretic Factor Expression: Synergism and Repression with Nkx2.5, *J. Biol. Chem. 278*, 22437−22445.
24. Cox, C. J., Espinoza, H. M., McWilliams, B., Chappell, K., Morton, L., Hjalt, T. A., Semina, E. V., and Amendt, B. A. (2002) Differential Regulation of Gene Expression by PITX2 Isoforms, *J. Biol. Chem. 277*, 25001−25010.
25. Saadi, I., Kuburas, A., Engle, J. J., and Russo, A. F. (2003) Dominant Negative Dimerization of a Mutant Homeodomain Protein in Axenfeld-Rieger Syndrome, *Mol. Cell. Biol. 23*, 1968−1982.
26. Liu, C., Liu, W., Lu, M., Brown, N. A., and Martin, J. F. (2001) Regulation of left-right asymmetry by thresholds of Pitx2c activity, *Development 128*, 2039−2048.
27. Liu, W., Selever, J., Lu, M. F., and Martin, J. F. (2003) Genetic dissection of *Pitx2* in craniofacial development uncovers new functions in branchial arch morphogenesis, late aspects of tooth morphogenesis and cell migration, *Development 130*, 6375−6385.
28. Semina, E. V., Reiter, R. S., and Murray, J. C. (1998) A new human homeobox gene OG12X is a member of the most conserved homeobox gene family and is expressed during heart development in mouse, *Hum. Mol. Genet. 7*, 415−422.
29. Amendt, B. A., and Semina, E. V., Alward, W. L. M. (2000) Rieger Syndrome: A Clinical, Molecular and Biochemical Analysis, *Cell. Mol. Life Sci. 57*, 1652−1666.
30. Coqueret, O., Berube, G., and Nepveu, A. (1996) DNA Binding by Cut Homeodomain Proteins Is Down-modulated by Protein Kinase C, *J. Biol. Chem. 271*, 24862−24868.
31. Karin, M. (1994) Signal transduction from the cell surface to the nucleus through the phosphorylation of transcription factors, *Curr. Opin. Cell Biol. 6*, 415−424.
32. Arias, J., Alberts, A. S., Brindle, P., Claret, F. X., Smeal, T., Karin, M., Feramisco, J., and Montminy, M. (1994) Activation of cAMP and mitogen responsive genes relies on a common nuclear factor, *Nature 370*, 226−229.
33. Kwok, R. P., Lundblad, J. R., Chrivia, J. C., Richards, J. P., Bachinger, H. P., Brennan, R. G., Roberts, S. G., Green, M. R., and Goodman, R. H. (1994) Nuclear protein CBP is a coactivator for the transcription factor CREB, *Nature 370*, 223−226.
34. Kidd, S. (1992) Characterization of the Drosophila cactus locus and analysis of interactions between cactus and dorsal proteins, *Cell 71*, 623−635.
35. Hug, H., and Sarre, T. F. (1993) Protein kinase C isoenzymes: divergence in signal transduction, *Biochem. J. 291*, 329−343.

36. Nishizuka, Y. (1992) Intracellular signaling by hydrolysis of phospholipids and activation of protein kinase C, *Science 258*, 607−614.
37. Selbie, L. A., Schmitz-Peiffer, C., Sheng, Y., and Biden, T. J. (1993) Molecular cloning and characterization of PKC iota, an atypical isoform of protein kinase C derived from insulin-secreting cells, *J. Biol. Chem. 268*, 24296−24302.
38. Akimoto, K., Mizuno, K., Osada, S., Hirai, S., Tanuma, S., Suzuki, K., and Ohno, S. (1994) A new member of the third class in the protein kinase C family, PKC lambda, expressed dominantly in an undifferentiated mouse embryonal carcinoma cell line and also in many tissues and cells, *J. Biol. Chem. 269*, 12677−12683.
39. Dekker, L. V., and Parker, P. J. (1994) Protein kinase C—a question of specificity, *Trends Biochem. Sci. 19*, 73−77.
40. Toker, A., Meyer, M., Reddy, K. K., Falck, J. R., Aneja, S., Parra, A., Burns, D. J., Ballas, L. M., and Cantley, L. C. (1994) Activation of protein kinase C family members by the novel polyphosphoinositides PtdIns-3,4-P2 and PtdIns-3,4,5-P3, *J. Biol. Chem. 269*, 32358−32367.
41. Johannes, F. J., Prestle, J., Eis, S., Oberhagemann, P., and Pfizenmaier, K. (1994) PKCu is a novel, atypical member of the protein kinase C family, *J. Biol. Chem. 269*, 6140−6148.
42. Wetsel, W. C., Khan, W. A., Merchenthaler, I., Rivera, H., Halpern, A. E., Phung, H. M., Negro-Vilar, A., and Hannun, Y. A. (1992) Tissue and Cellular Distribution of the Extended Family of Protein Kinase C Isoenzymes, *J. Cell Biol. 117*, 121−133.
43. Nishikawa, K., Toker, A., Johannes, F.-J., Songyang, Z., and Cantley, L. C. (1997) Determination of the Specific Substrate Sequence Motifs of Protein Kinase C Isozymes, *J. Biol. Chem. 272*, 952−960.
44. Pearson, R. B., and Kemp, B. E. (1991) Protein Kinase Phosphorylation Site Sequences and Consensus Specificity Motifs: Tabulations, *Methods Enzymol. 200*, 62−79.
45. Brooks, B. P., Moroi, S. E., Downs, C. A., Wiltse, S., Othman, M. I., Semina, E. V., and Richards, J. E. (2004) A Novel Mutation in the PITX2 Gene in a Family with Axenfeld-Rieger Syndrome, *Ophthalmic Genetics*, in press.
46. Amendt, B. A., Hesslein, D., Chang, L.-J., and Stoltzfus, C. M. (1994) Presence of negative and positive cis-acting RNA splicing elements within and flanking the first tat coding exon of the human immunodeficiency virus type 1, *Mol. Cell. Biol. 14*, 3960−3970.
47. Amendt, B. A., and Stoltzfus, C. M. (1995a) Presence of exon splicing silencers within human immunodeficiency virus type 1 *tat* exon 2 and *tat-rev* exon 3: Evidence for inhibition mediated by cellular factors, *Mol. Cell. Biol. 15*, 4606−4615.
48. Gage, P. J., Suh, H., and Camper, S. A. (1999a) The bicoid-related Pitx gene family in development, *Mamm. Genome 10*, 197−200.
49. Bulfone, A., Kim, H.-J., Puelles, L., Porteus, M. H., Grippo, J. F., and Rubenstein, J. L. R. (1993) The mouse *Dlx-2* (*Tes-1*) gene is expressed in spatially restricted domains of the forebrain, face and limbs in midgestation mouse embryos, *Mech. Dev. 40*, 129−140.
50. Qiu, M., Bulfone, A., Ghattas, I., Meneses, J. J., Christensen, L., Sharpe, P. T., Presley, R., Pedersen, R. A., and Rubenstein, J. L. R. (1997) Role of the Dlx Homeobox Genes in Proximodistal Patterning of the Branchial Arches: Mutations of Dlx-1, Dlx-2, and Dlx-1 and -2 Alter Morphogenesis of Proximal Skeletal and Soft Tissue Structures Derived from the First and Second Arches, *Dev. Biol. 185*, 165−184.
51. Marino, J., Cook, P., and Miller, K. S. (2003) Accurate and statistically verified quantification of relative mRNA abundances using SYBR Green I and real-time RT-PCR, *J. Immunol. Methods 283*, 291−306.
52. Qiu, M., Bulfone, A., Martinez, S., Meneses, J. J., Shimamura, K., Pedersen, R. A., and Rubenstein, J. L. R. (1995) Null mutation of Dlx-2 results in abnormal morphogenesis of proximal first and second branchial arch derivatives and abnormal differentiation in the forebrain, *Genes Dev. 9*, 2523−2538.
53. Robinson, G. W., and Mahon, K. A. (1994) Differential and overlapping expression domains of Dlx-2 and Dlx-3 suggest distinct roles for Distal-less homeobox genes in craniofacial development, *Mech. Dev. 48*, 199−215.
54. Thomas, B. L., Porteus, M. H., Rubenstein, J. L., and Sharpe, P. T. (1995) The spatial localization of Dlx-2 during tooth development, *Connect. Tissue Res. 32*, 27−34.
55. Thomas, B. L., Liu, J. K., Rubenstein, J. L. R., and Sharpe, P. T. (2000) Independent regulation of Dlx2 expression in the epithelium and mesenchyme of the first branchial arch, *Development 127*, 217−224.
56. Espinoza, H. M., Cox, C. J., Semina, E. V., and Amendt, B. A. (2002) A molecular basis for differential developmental anomalies in Axenfeld-Rieger syndrome, *Hum. Mol. Genet. 11*, 743−753.
57. Kasahara, H., and Izumo, S. (1999) Identification of the In Vivo Casein Kinase II Phosphorylation Site within the Homeodomain of the Cardiac Tissue-Specifying Homeobox Gene Product Csx/Nkx2.5, *Mol. Cell. Biol. 19*, 526−536.
58. Smidt, M. P., Cox, J. J., van Schaick, H. S. A., Coolen, M., Schepers, J., van der Kleij, A. M., and Burbach, J. P. H. (2000) Analysis of Three Ptx2 Splice Variants on Transcriptional Activity and Differential Expression Pattern in the Brain, *J. Neurochem. 75*, 1818−1825.
59. Augustijn, K. D., Duval, D. L., Wechselberger, R., Kaptein, R., Gutierrez-Hartmann, A., and van der Vliet, P. C. (2002) Structural characterization of the PIT-1/ETS-1 interaction: PIT-1 phosphorylation regulates PIT-1/ETS-1 binding, *PNAS 99*, 12657−12662.
60. Bradford, A. P., Brodsky, K. S., Diamond, S. E., Kuhn, L. C., Liu, Y., and Gutierrez-Hartmann, A. (2000) The Pit-1 homeodomain and beta-domain interact with Ets-1 and modulate activation of the rat prolactin promoter, *J. Biol. Chem. 275*, 3100−3106.
61. Bawden, J. W., Rozell, B., Wurtz, T., Fouda, N., and Hammarstrom, L. (1994) Distribution of Protein Kinase Ca and Accumulation of Extracellular Ca^{+} During Early Dentin and Enamel Formation, *J. Dent. Res. 73*, 1429−1436.
62. Mucchielli, M.-L., Mitsiadis, T. A., Raffo, S., Brunet, J.-F., Proust, J.-P., and Goridis, C. (1997) Mouse Otlx2/RIEG Expression in the Odontogenic Epithelium Precedes Tooth Initiation and Requires Mesenchyme-Derived Signals for Its Maintenance, *Dev. Biol. 189*, 275−284.
63. St. Amand, T. R., Zhang, Y., Semina, E. V., Zhao, X., Hu, Y., Nguyen, L., Murray, J. C., and Chen, Y. (2000) Antagonistic Signals between BMP4 and FGF8 Define the Expression of Pitx1 and Pitx2 in Mouse Tooth-Forming Anlage, *Dev. Biol. 217*, 323−332.
64. Mischak, H., Pierce, J. H., Goodnight, J., Kazanietz, M. G., Blumberg, P. M., and Mushinski, J. F. (1993) Phorbol ester-induced myeloid differentiation is mediated by protein kinase C-alpha and -delta and not by protein kinase C-beta II, -epsilon, -zeta, and -eta, *J. Biol. Chem. 268*, 20110−20115.
65. Nakamura, S., and Nishizuka, Y. (1994) Lipid mediators and protein kinase C activation for the intracellular signaling network, *J. Biochem (Tokyo) 115*, 1029−1034.
66. Nakanishi, H., and Exton, J. H. (1992) Purification and characterization of the zeta isoform of protein kinase C from bovine kidney, *J. Biol. Chem. 267*, 16347−16354.
67. Goodnight, J. A., Mischak, H., Kolch, W., and Mushinski, J. F. (1995) Immunocytochemical localization of eight protein kinase C isozymes overexpressed in NIH 3T3 fibroblasts. Isoform-specific association with microfilaments, Golgi, endoplasmic reticulum, and nuclear and cell membranes, *J. Biol. Chem. 270*, 9991−10001.
68. Goodnight, J., Mischak, H., and Mushinski, J. F. (1994) Selective involvement of protein kinase C isozymes in differentiation and neoplastic transformation, *Adv. Cancer Res. 64*, 159−209.

BI048362X